Effect of Plasticizers in Poly(vinyl alcohol)-Based Hybrid Solid Polymer Electrolytes

S. Rajendran, M. Sivakumar, R. Subadevi

Department of Physics, Alagappa University, Karaikudi 630 003, India

Received 17 January 2003; accepted 17 March 2003

ABSTRACT: Hybrid solid polymer electrolyte films consisting of poly(vinyl alcohol) (PVA), poly(methyl methacrylate) (PMMA), $LiBF_4$, and ethylene carbonate/propylene carbonate (EC/PC) were prepared with a solvent-casting technique. The complexation was investigated with Fourier transform infrared and X-ray diffraction. The ionic conductivities of the electrolyte films were determined with an alternating-current impedance technique for various temperatures in the range of 302–373 K. The maximum conductivity value, 1.2886×10^{-3} S/cm, was observed for a PVA–PMMA–$LiBF_4$–EC complex. Thermogravimetry/differential thermal analysis was performed to ascertain the thermal stability of the electrolyte with the maximum conductivity value. For an examination of the cyclic and reversible performance of the film, a cyclic voltammetry study was carried out. The surface morphology of the EC-and PC-based electrolytes was examined with scanning electron microscopy.
 J Appl Polym Sci 90: 2794–2800, 2003

Key words: poly (vinyl alcohol); XRD; FT-IR; TG/DTA

INTRODUCTION

Extensive work has been carried out for about a decade to develop an all-solid-state battery based on the use of thin plastic films.[1,2] Currently, much effort is being invested in the development of solid-state lithium rechargeable batteries.[3,4] Several methods, such as copolymerization,[5] plasticization,[6] blending,[7] and the addition of ceramic fillers,[8] are in use to modulate the conductivity of polymer electrolytes. Among the various methods used to produce high ionic conduction, polymer blends constitute the most feasible and promising approach. When two or more polymers give rise to a homogeneous mixture, a miscible or compatible blend is formed in which one polymer is adopted to absorb the electrolyte active species, whereas the other remains an undissolved, inert second phase providing toughness to the electrolyte films. The blending technique was exemplified by Faria and Moreira,[9] who studied the kinetics, structural transitions, and dielectric behavior of poly (vinylidene fluoride-co-trifluoro ethylene) (PVdF–TrFE)/poly(methyl methacrylate) (PMMA) blends.

Since the advent of solid polymer electrolytes, poly(ethylene oxide) has been by far the most often chosen polymer matrix for lithium-ion conductors because of its easy availability and the high ionic conductivities of the polymer–salt systems below 100°C. However, it has poor mechanical strength in the high conduction region,[10] which is overcome by poly(vinyl alcohol) (PVA)-based electrolytes for their potential applications in electric double-layer capacitors, sensors, electrochromic windows, and so forth.[11–13] It has a carbon chain backbone with hydroxy groups attached to methane carbons that acts as a source of hydrogen bonding and, therefore, assistance in the formation of polymer blends.[14–17] Kanbara et al.[18] studied PVA-based electrolytes complexed with lithium salts for applications in electric double-layer capacitors. Chandrasekaran et al.[19] reported the electrical conductivity of PVA–$NaClO_3$ electrolytes to be 10^{-6} S/cm. The conductivity of PVA polymer complexes also shows high values through the blending of PVA with other suitable polymers. PMMA is compatible with other polymers. Iijima et al.[20] first reported about PMMA, and even more recently, Bohnke et al.[21] and Appetecchi[22] studied the kinetics and stability of lithium electrodes in PMMA-based gel electrolytes. The compatibility between PVA and PMMA polymer blends in solution was reported by Singh and Singh,[23] who used ultrasonic and viscometric techniques.

An attempt was made to plasticize a PVA(15)–PMMA(10)–$LiBF_4$(8) polymer electrolyte system with the plasticizers ethylene carbonate (EC) and propylene carbonate (PC) and a mixture of them. The plasticizers were chosen because of their high dielectric constants (89.6 and 64.4), high boiling points (242 and 248°C), and low vapor pressures (36.5 and −55°C).[24] The ionic conductivities of plasticized PVA(15)–PMMA(10)–$LiBF_4$(8) systems were determined. The electrolyte films were characterized with X-ray diffraction (XRD), Fourier transform infrared (FTIR), thermogravimetry/

Correspondence to: S. Rajendran (sraj54@yahoo.com).

Journal of Applied Polymer Science, Vol. 90, 2794–2800 (2003)

differential thermal analysis (TG/DTA), cyclic voltammetry (CV), and scanning electron microscopy (SEM), and the results are reported.

EXPERIMENTAL

PVA with an average molecular weight of 115,000 (BDH, Poole, England), PMMA with an average molecular weight of 120,000 (Aldrich, Milwaukee, WI), the inorganic salt $LiBF_4$, and EC (E-Merck, Hohenbrunn, Germany) were used in this study. PVA, PMMA, and $LiBF_4$ were dried before use in a Logitech DTC 5050 vacuum oven (Bangalore, India) at 100, 90, and 80°C, respectively, under 10^{-3} Torr of pressure for 10 h. The plasticizer EC was used without further purification. When the melting temperature is closer to the decomposition of the polymers, a solvent-casting technique is preferred for casting the films because this process reduces the energy for melting.[25] In this study, hybrid solid polymer electrolytes (HSPEs) containing EC and PC in ratios of 67:0, 50:17, 17:50, and 0:67, complexed with PVA(15)–PMMA(10)–$LiBF_4$(8), were prepared with a solvent-casting technique.

These compositions of the lithium salt, EC, PC, PVA, and PMMA were dissolved in distilled dimethylformamide (DMF; Merck). The solution was stirred and heated continuously at 70°C for several hours until the mixture became a homogeneous gel. The film was cast by the spreading of the suspension on a glass plate and in Teflon bushes. DMF was allowed to evaporate slowly. Finally, the film was dried at 85°C in a vacuum oven under 10^{-3} Torr of pressure for 4–5 h for the removal of further traces of DMF. The resulting film was visually examined for its dryness and freestanding nature. Chemical storage, film casting, and cell assemblies were performed in a vacuum atmosphere.

The structure of the resultant electrolyte films was investigated with a JEOL JDX 8030 X-ray diffractometer (Tokyo, Japan). The fundamental vibrations of the polymer complexes were studied by FTIR analysis in the range of 4000–400 cm^{-1} with a PerkinElmer 577 IR spectrometer (Norwalk, CT).

The bulk electrical conductivity of the electrolyte was measured by sandwiching the polymer electrolyte between stainless steel (SS) electrodes. To avoid film contamination from moisture, we performed the conductivity measurements *in vacuo*. The measurements were made with a Keithley LCZ 3330 meter (Cleveland, OH). The conductivity values were evaluated from complex impedance plots in the temperature range of 302–373 K.

The thermal stability of the electrolyte with a higher conductivity value was studied with a TG/DTA apparatus (STA 1500, PL Thermal Sciences, Surrey, UK). The sample was put in an aluminum pan and was heated at a rate of 10°C/min up to 700°C. TG and DTA curves were recorded. To investigate the cyclability and reversibility of the electrolyte film, we performed CV studies with an EG&G 6310 impedance analyzer (Princeton Applied Research, Oak Ridge, TN). The surface morphology of the electrolyte films was examined with a Hitachi S3000H scanning electron microscope (Japan).

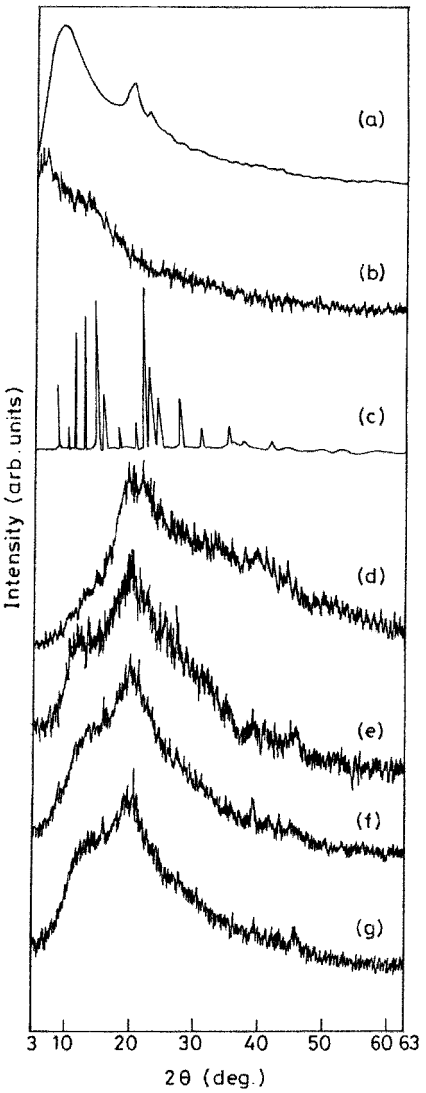

Figure 1 XRD patterns of (a) PVA, (b) PMMA, (c) $LiBF_4$, (d) PVA(15)–PMMA(10)–$LiBF_4$(8)–EC(67), (e) PVA(15)–PMMA(10)–$LiBF_4$(8)–EC(50):PC(17), (f) PVA(15)–PMMA(10)–$LiBF_4$(8)–EC(17):PC(50), and (g) PVA(15)–PMMA(10)–$LiBF_4$(8)–PC(67).

RESULTS AND DISCUSSION

XRD analysis

The XRD patterns are shown in Figure 1(a–g). Some distinctive features of the patterns are as follows:

1. Figure 1(a–c) shows the XRD patterns of pure PVA, PMMA, and $LiBF_4$, and the degrees of crys-

tallinity were estimated to be 2.84, 0.96, and 42.55%, respectively. The diffraction patterns of complexes containing EC and PC in ratios of 67:0, 50:17, 17:50, and 0:67, complexed with a PVA(15)–PMMA(10)–$LiBF_4$(8) system, are shown in Figure 1(d–g). Their respective degrees of crystallinities were estimated to be 0.77, 1.71, 1.94, and 2.06%.

2. The maximum conductivity value, 1.2886×10^{-3} S/cm, was obtained for the PVA(15)–PMMA(10)–$LiBF_4$(8)–EC(67) system in agreement with the lower degree of crystallinity, 0.77%, as compared to the degrees of the other systems.
3. The diffraction peak at $2\theta = 19.5°$ in pure PVA was absent in the complexes, and that at $2\theta = 22°$ in PVA was slightly shifted in the complexes.
4. No peaks pertaining to $LiBF_4$ were present in the complexes, and this indicated the complete dissolution of the salt in the polymer matrix and, therefore, the complexation.

These XRD patterns reveal that the addition of the plasticizers EC and PC reduced the crystallinity considerably. The plasticizers may have induced significant disorder into the original polymer,[26] and this is attributed to the interactions between the polymer and the solvents, which resulted in polymer electrolytes with much lower crystallinity than that manifested in the diffraction peaks.

FTIR studies

IR was used to characterize the chain structures of the polymers and led the way in interpreting the reactions of the multifunctional monomers, including rearrangements and complexation. The IR spectra of PVA, PMMA, $LiBF_4$, EC, and PC, as well as the complexes, are shown in Figure 2(a–i).

The most important band of alcohols and phenols is the hydroxyl (O—H) band. It appears at 3575 cm^{-1} in pure PVA and is displaced toward the lower wave number in the complexes. This confirms the specific interactions in the polymer matrices. The asymmetric CH_2 stretching and aliphatic C—H stretching of PVA appearing at 2925 cm^{-1} is shifted to 2934 cm^{-1} in the complexes. The vibrational peak at 1100 cm^{-1}, assigned to C—O stretching of the secondary alcohol of PVA, is shifted to 1106 cm^{-1} in film E4 and to 1097 cm^{-1} in the remaining films. For PVA,[27] absorptions at 916 and 1141 cm^{-1} were found to be characteristic of the syndiotactic structure after the isotactic polymer was prepared. The absorption peak at 916 cm^{-1} is shifted to 902 cm^{-1} in film E1 and to 912 cm^{-1} in the remaining films. The peak appearing at 1141 cm^{-1} is absent in the complexes. The band at 1260 cm^{-1} assigned to C—C stretching of PVA, is shifted to 1247 cm^{-1} in the complexes.

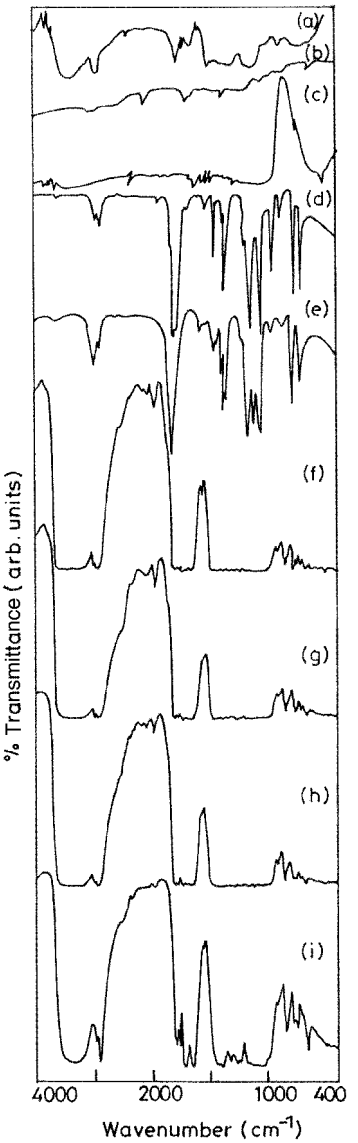

Figure 2 FTIR spectra of (a) PVA, (b) PMMA, (c) $LiBF_4$, (d) EC, (e) PC, (f) PVA(15)–PMMA(10)–$LiBF_4$(8)–EC(67), (g) PVA(15)–PMMA(10)–$LiBF_4$(8)–EC(50):PC(17), (h) PVA(15)–PMMA(10)–$LiBF_4$(8)–EC(17):PC(50), and (i) PVA(15)–PMMA(10)–$LiBF_4$(8)–PC(67).

The vibrational peak at 1736 cm^{-1}, assigned to C═O stretching of PMMA,[28] is shifted to 1731 cm^{-1} in the complexes. The O—CH_2 asymmetric stretching and C—O stretching of PMMA appearing at 3010 and 1280 cm^{-1} are shifted to 3000 and 1276 cm^{-1}, respectively, in the complexes. The characteristic vibrational peaks at 1452, 1173, and 750 cm^{-1} are assigned to CH_2 scissoring, twisting, and rocking modes of PMMA, which are shifted to 1440, 1190, and 751 cm^{-1} in the complexes. The CH_2 wagging of PMMA appearing at 947 cm^{-1} is absent in the complexes. The absorption bands at 1063 and 1377 cm^{-1}, correlated with the

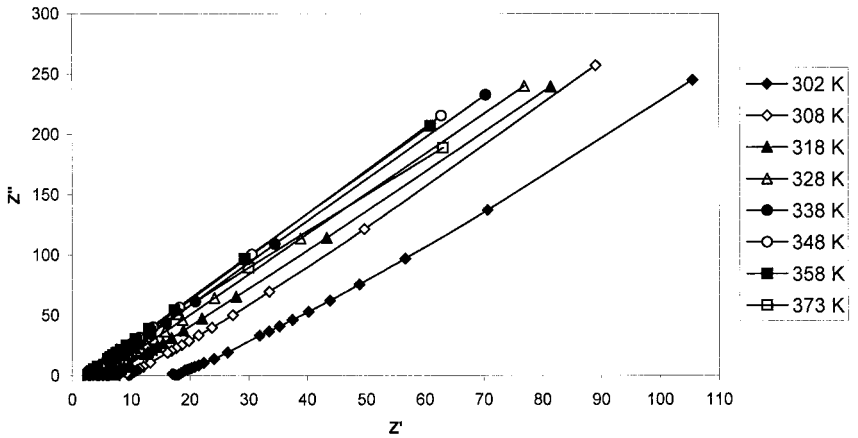

Figure 3 Complex impedance plot of the PVA(15)–PMMA(10)–$LiBF_4$(8)–EC(67) system from 302 to 373 K.

syndiotactic pairs of PMMA,[29] are absent in the complexes. The peaks pertaining to PMMA at 2360, 840, 668, and 483 cm^{-1} are shifted to 2363, 845, 665, and 479 cm^{-1} in the complexes.

The characteristic vibrational band of $LiBF_4$ appearing at 510 cm^{-1} is assigned to BF_4^-. This is shifted to 522 cm^{-1} in all the complexes, and this is evidence of the polymer–salt interactions. The vibrational peak at 1810 cm^{-1} is assigned to the $\nu_{C=O}$ region of EC and PC.[30] It occurs at 1807 cm^{-1} in film E1 and at 1803 cm^{-1} in the remaining films. One of the significant bands occurring in the $\nu_{C=O}$ region is due to a fermi resonance of skeletal breathing around 1788 cm^{-1}. This is shifted to 1770 cm^{-1} in film E1 and to 1776 cm^{-1} in the remaining films. This downward shift of $\nu_{C=O}$ of carbonate to 1770 cm^{-1} indicates the interaction of the plasticizer with $LiBF_4$ on complexation. The peak pertaining to EC and PC appearing at 772 cm^{-1} is shifted to 776 cm^{-1} in the complexes.

The vibrational peaks at 3698, 3431, and 1410 cm^{-1} of PVA, 2954, 1542, 1508, 1384, 1149, and 990 cm^{-1} of PMMA, 3563, 1305, 1633, and 1056 cm^{-1} of $LiBF_4$, 1475, 1401, 1383, 1156, 971, and 885 cm^{-1} of EC, and 1385, 1360, 1125, 1055, and 954 cm^{-1} of PC are absent in the complexes. This analysis establishes the formation of polymer–salt complexes.

Conductivity studies

The ionic conductivity of the electrolyte was calculated with the relation $\sigma = l/R_bA$, where σ is the conductivity, l is the thickness, R_b is the bulk resistance, and A is the area of the electrolyte. A typical complex impedance plot of the PVA(15)–PMMA(10)–$LiBF_4$(8)–EC(67) system (film E1) for various temperatures is shown in Figure 3. The disappearance of the semicircular portion in the high-frequency region of the complex impedance plot indicates that the conductivity was mainly due to the ions.[31]

The maximum conductivity value (1.2886×10^{-3}S/cm) was obtained for film E1 at 302 K (Table I). This value was higher than the values reported in the range of 10^{-8} to 10^{-4} S/cm for PVA–PMMA–$LiClO_4$–dimethylphthalate (DMP) and PVA–$LiCF_3SO_3$ systems.[32,33] The maximum conductivity value for film E1 may be due to the higher dielectric constant of EC, which dissolved enough charge carriers and provided a more mobile medium for the ions so as to enhance the conductivity behavior of the resultant films.[34] The variation of the log conductivity with the inverse absolute temperature for various complexes is presented in Figure 4. The nonlinearity of the plots suggests that ion transport in polymer electrolytes is related to the segmental motion of the polymers. As the temperature increased, the conductivity also increased, and this behavior is in agreement with the theory.[35]

TG/DTA

The TG/DTA curve for film E1 is shown in Figure 5. Mishra and Rao[36] reported that in pure PVA, decom-

TABLE I
σ Values for the PVA–PMMA–$LiBF_4$–EC:PC Systems

	σ value for PVA–PMMA–$LiBF_4$–EC:PC complex ($\times 10^{-3}$ S/cm)							
EC:PC Compositions	302 K	308 K	318 K	328 K	338 K	348 K	358 K	373 K
67:0 (E1)	1.2886	2.3229	3.2850	4.5019	5.8933	7.5472	8.7892	9.0377
50:17 (E2)	0.5978	0.6824	1.0015	1.5983	1.8264	2.4388	2.9904	3.5017
17:50 (E3)	0.5379	0.6744	0.9015	1.4335	1.6586	2.1231	2.4389	2.9918
0:67 (E4)	0.4648	0.5775	0.8517	1.2376	1.6287	1.9079	2.1301	2.4855

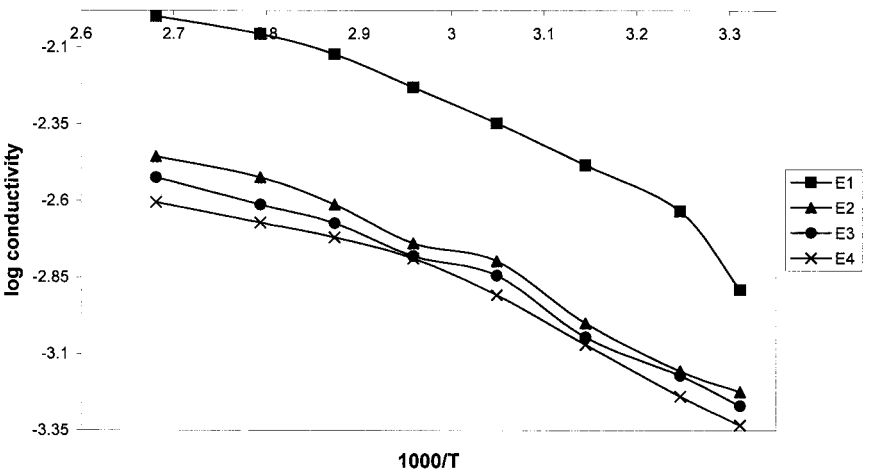

Figure 4 Arrhenius plot of PVA–PMMA–$LiBF_4$–EC:PC complexes.

position occurred in two stages, and it was thermally stable up to 265°C. In this study, it was observed from the TG curve that the first decomposition occurred at 336°C, with a gradual weight loss of 26%. The complete decomposition of the film took place between 600 and 618°C with corresponding weight losses of 77 and 83%, respectively.

Endothermic peaks at 387, 404, and 510°C and exothermic peaks at 379, 421, 479, 540, and 612°C were observed in the DTA curve. The first decomposition occurred from 336 to 435°C and was accompanied by two large exothermic peaks at 379 and 421°C. A sharp and large exothermic peak at 612°C, concurrent with an appreciable weight loss of about 82%, took place, indicating the complete decomposition of the film, which was evidenced by the TG curve. From this discussion, it can be concluded that the thermal stability of the polymer electrolyte film E1 was 336°C.

CV

A cyclic voltammogram of film E1 is presented in Figure 6. CV was performed for the SS/polymer electrolyte/SS cell couple at a scanning rate of 5 mV/s. CV studies employing SS electrodes were previously carried out by Kumar and Munichandraiah[37] for polymer electrolytes based on PMMA. The following points were observed with CV:

1. An electrochemical window was obtained from −1000 to +1000 mV for a PVA–PMMA–$LiBF_4$–EC polymer electrolyte.
2. The cathodic and anodic peaks were not observed, and this may be due to the noninteraction of lithium in the polymer electrolyte with the SS electrodes.

The cyclic voltammogram strongly demonstrated the good reversibility and cyclability of the polymer electrolyte film.

SEM studies

SEM micrographs of films E1 and E4 are shown in Figure 7(a,b). Figure 7(a) shows the increased dis-

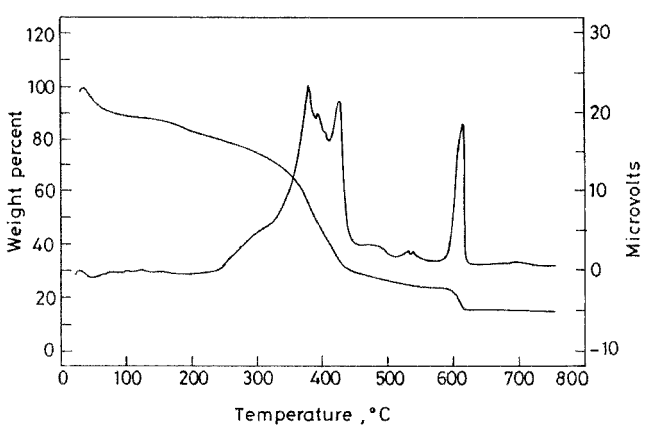

Figure 5 TG/DTA curves for the PVA(15)–PMMA(10)–$LiBF_4$(8)–EC(67) complex.

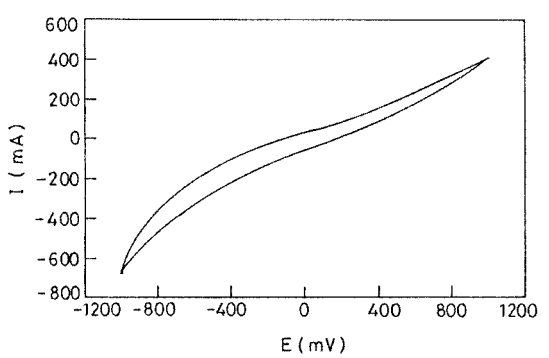

Figure 6 Cyclic voltammogram of the PVA(15)–PMMA(10)–$LiBF_4$(8)–EC(67) complex with SS electrodes (scanning rate = 5 mV/s).

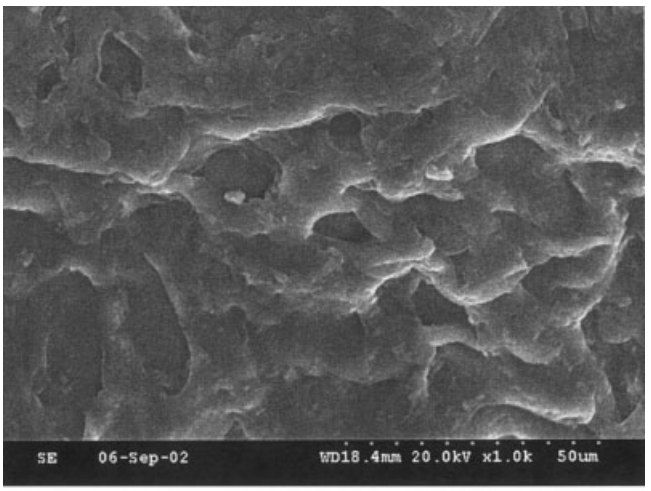

(a)

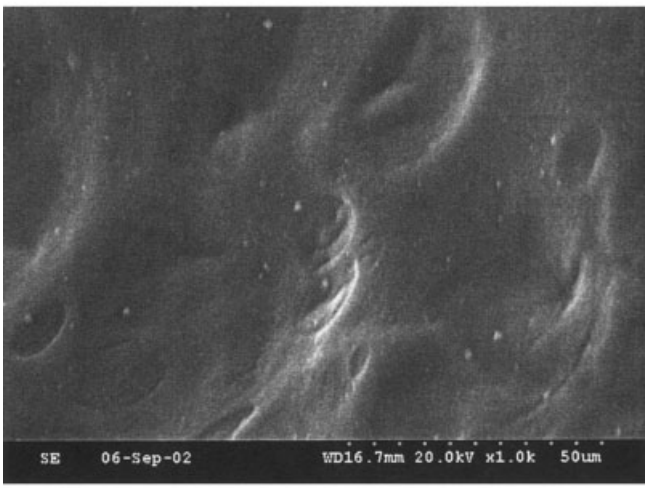

(b)

Figure 7 SEM images of (a) PVA(15)–PMMA(10)–$LiBF_4$(8)–EC(67) and (b) PVA(15)–PMMA(10)–$LiBF_4$(8)–PC(67) polymer complexes (1000× magnification).

persed medium for which the maximum conductivity was obtained.

CONCLUSION

1. Flexible and freestanding HSPEs consisting of PVA–PMMA–$LiBF_4$–EC:PC were prepared with a solvent-casting technique.
2. The complex formation between the polymer and salt was corroborated with FTIR and XRD analyses.
3. The ionic conductivity of the prepared electrolyte films was measured with an alternating-current impedance technique. The maximum conductivity value, 1.2886×10^{-3} S/cm, was obtained for a PVA(15)–PMMA(10)–$LiBF_4$(8)–EC(67) complex (film E1), and this may have been due to the dielectric constant of EC being higher than that of PC.
4. The thermal stability of polymer electrolyte film E1 was ascertained with TG/DTA to be 336°C.
5. The cyclic and reversible performances of film E1 were studied.

Because the polymer electrolyte system PVA(15)–PMMA(10)–$LiBF_4$(8)–EC(67) has the maximum conductivity value among the four systems studied, it can be used as an electrolyte in the fabrication of Li batteries. It also exhibits good thermal stability and cyclability, as shown by TG/DTA and CV studies.

References

1. Choi, N. S.; Park, J. K. Electrochim Acta 2001, 46, 1453.
2. Armand, M. B. Adv Mater Res 1990, 2, 278.
3. Gauthier, M. J Electrochem Soc 1985, 132, 1333.
4. Munshi, M. Z. A.; Owens, B. B. Solid State Ionics 1988, 26, 41.
5. Kim, D. W.; Park, J. R.; Rhee, H. W. Solid State Ionics 1996, 83, 49.
6. Wieckzorek, W.; Stevens, J. R. J Phys Chem B 1997, 101, 1529.
7. Przyluski, J.; Wieczorek, W. Solid State Ionics 1989, 36, 165.
8. Cherng, J. Y.; Munshi, M. Z. A.; Owens, B. B.; Smyrl, W. H. Solid State Ionics 1988, 28, 857.
9. Faria, L. O.; Moreira, R. L. J Polym Sci Part B: Polym Phys 2000, 38, 34.
10. Rajendran, S.; Uma, T. J Power Sources 2000, 87, 218.
11. Wang, B.; Mukataka, S.; Kokufuta, E.; Ogiso, M.; Kodama, M. J Polym Sci Part B: Polym Phys 2000, 38, 214.
12. Masuda, K.; Kaji, H.; Horii, F. J Polym Sci Part B: Polym Phys 2000, 38, 1.
13. Armand, M. B. In Polymer Electrolytes I; MacCallum, J. A.; Vincent, C. A., Eds.; Elsevier: London, 1987.
14. Coleman, M. M.; Painter, P. C. Prog Polym Sci 1995, 20, 1.
15. Lee, J. H.; Lee, H. B.; Andrade, J. D. Prog Polym Sci 1995, 20, 1043.
16. Pearce, E. M.; Kwei, T. K.; Min, B. Y. J Macromol Sci Chem 1984, 21, 1181.
17. Robsen, L. M.; Hale, W. F.; Merriam, C. N. Macromolecules 1981, 14, 1644.
18. Kanbara, T.; Inami, M.; Yamamoto, T. J Power Sources 1991, 36, 87.
19. Chandrasekaran, R.; Mangani, I. R.; Vasanthi, R.; Selladurai, S. Bull Electrochem 2001, 17, 249.
20. Iijima, T.; Toyoguchi, Y.; Eda, N. Denki Kogaku 1985, 53, 619.
21. Bohnke, O.; Frand, G.; Rezrazi, M.; Rousselot, C.; Truche, C. Solid State Ionics 1993, 66, 97.
22. Appetecchi, G. B. Electrochim Acta 1995, 140, 997.
23. Singh, Y. P.; Singh, R. P. Eur Polym J 1983, 19, 535.
24. Tsuchida, E.; Ohno, H.; Tsunemi, K. Electrochim Acta 1983, 28, 591.
25. Encyclopedia of Polymer Science and Engineering; Mark, H. F., Ed.; Wiley-Interscience: New York, 1964; Vol. 1.

26. Hay, J. N. In Analysis of Polymer Systems; Bark, L. S.; Allen, N. S., Eds.; Applied Science: London, 1982.
27. Murahashi, S.; Yuki, H. J Polym Sci 1962, 62, S77.
28. Rajendran, S.; Mahendran, O.; Kannan, R. J Phys Chem Solids 2002, 63, 303.
29. Nyquist, R. A. Infrared Spectra of Plastics and Resins; Dow Chemical: Midland, MI, 1960.
30. Nyquist, R. A.; Settineri, S. E. Appl Spectrosc 1991, 45, 1991.
31. Jacob, M. M. E.; Prabaharan, S. R. S.; Radhakrishna, S. Solid State Ionics 1997, 104, 267.
32. Rajendran, S.; Mahendran, O. Ionics 2001, 7, 463.
33. Every, H. A.; Zhou, F.; Forsyth, M.; MacFarlane, D. R. Electrochim Acta 1998, 43, 1465.
34. MacCallum, J. A.; Vincent, C. A. Polymer Electrolyte Reviews I; Elsevier: London, 1987.
35. Armand, M. B.; Chabagno, J. M.; Duclot, M. J. In Fast-Ion Transport in Solids; Vashishta, P.; Mundy, L. N.; Shenoy, G., Eds.; North Holland: Amsterdam, 1979; p 131.
36. Mishra, R.; Rao, K. J. Eur Polym J 1999, 35, 1883.
37. Kumar, G. G.; Munichandraiah, N. Electrochim Acta 2002, 47, 1013.